The shallow magma pathway geometry at Mt. Etna volcano

D. Patanè
Istituto Nazionale di Geofisica e Vulcanologia, Sezione di Catania, P.zza Roma 2, 95123 Catania, Italy

G. Di Grazia
Istituto Nazionale di Geofisica e Vulcanologia, Sezione di Catania, P.zza Roma 2, 95123 Catania, Italy

A. Cannata
Dipartimento di Scienze Geologiche, Università di Catania, Corso Italia 57, 95129 Catania, Italy

P. Montalto
Istituto Nazionale di Geofisica e Vulcanologia, Sezione di Catania, P.zza Roma 2, 95123 Catania, Italy
Dipartimento di Ingegneria Elettrica, Elettronica e dei Sistemi, Università di Catania, Viale Andrea Doria 6, 95125 Catania, Italy

E. Boschi
Istituto Nazionale di Geofisica e Vulcanologia, Sezione di Catania, P.zza Roma 2, 95123 Catania, Italy

Abstract

A fundamental goal of volcano seismology is to understand the dynamics of active magmatic systems in order to assess eruptive behavior and the associated hazard. Imaging of magma conduits, quantification of magma transport and investigation of long-period seismic sources, together with their temporal variations, are crucial for the comprehension of eruption-triggering mechanisms.

At Mt. Etna volcano, several intense episodes of tremor activity were recorded during 2007, in association with strombolian activity and/or intense fire fountaining episodes occurring from the South East Crater (SEC). The locations of the tremor sources and of the long-period seismic events are used here to constrain both the area and the depth range of magma degassing, highlighting the geometry of the shallow conduits feeding SEC. The imaged conduits consist of two connected resonating dike-like bodies, NNW-SSE and NW-SE oriented, extending from sea level to the surface. In addition, we show how tremor, long-period (LP) and very-long-period (VLP) event locations and signatures reflect pressure fluctuations in the plumbing system associated with the ascent/discharge of gas-rich magma linked to the lava fountains. The evidence here reported, also corroborated by ground deformation variations, can help develop a better prediction and early-warning system for those eruptions (effusive or explosive) that apparently manifest no clear precursors.

Index terms: 7280 Seismology: Volcano seismology (8419); 8419 Volcanology: Volcano monitoring (7280); 8494 Volcanology: Instruments and techniques.

Keywords: volcano plumbing system; volcanic tremor; LP and VLP events; Mt. Etna.

1.1 Introduction

Like many basaltic volcanoes, Mt. Etna typically erupts in effusive to weakly explosive styles, even though powerful explosive eruptions (sub-Plinian to Plinian events) have been recognized

during the Quaternary (Del Carlo et al., 2004). As a result, lava flow propagation has typically been considered the main hazard at Etna and only recently its explosive activity has been taken into account as a serious volcanic risk for local populations and for aviation in the central Mediterranean region (Andronico et al., 2007, 2008b). This because, in the last decades, explosive eruptions represented its most frequent activity, producing eruptive plumes and copious ash fallout on its flanks. Since the 1970's, more than 180 fire fountain episodes have occurred at summit craters (Behncke and Neri, 2003). During the 2001 and 2002-2003 eruptions, an exceptional and prolonged explosive activity was observed for the first time in the last century (Allard et al., 2006). These two highly explosive events were related to the arrival of undegassed, volatile-rich, fast-rising magma that rose from the deep portion of the feeding system and bypassed the central conduits (Andronico et al., 2008a; Patanè et al., 2003, 2006).

After the 2004-2005 quiet summit effusive eruption and the 2006 summit eruptive phase, characterized by both effusive and explosive activity from the South East Crater (SEC), a new period of explosive activity started from this crater at the end of March 2007, producing 4 episodes of fire fountains in about 1.5 months. Thereafter, on September 4-5, 2007, one of the most powerful fire fountaining episodes (both in terms of duration, about 12 hours, and erupted volume of lava and tephra, about 2-4 x 10^6 m^3) originated from the SEC, producing a plume up to 2 km-high and dispersed deposits up to several tens of km from the volcano (Andronico et al., 2008b). This was followed on November 23-24 by another energetic fire fountaining episode (roughly 6 hours long).

Both explosive and effusive eruptive styles are believed to be largely controlled by the total volatile content and magma flow rate (Woods and Cardoso, 1997), which is modulated by processes within the volcanic conduit (Jaupart and Vergniolle, 1988). Models for the ascent of magma through shallow conduits have become increasingly sophisticated over the last two decades (Jaupart and Vergniolle, 1988; Sahagian, 2005). However, constraining the model behavior with observational data has proven difficult because the geometry of the shallow volcanic plumbing system is not

generally well defined at almost all volcanoes worldwide, notwithstanding recent advances in the high-resolution seismic tomography studies (Chouet, 2003; Patanè et al., 2006).

Long-period seismic signals, including volcanic tremor and LP events, commonly observed on many volcanoes worldwide, are believed to be caused by fluids moving in volcanic conduits (Chouet, 1996; Almendros et al., 2002a) and considered precursory phenomenon for eruptive activity (Chouet, 1996). The possibility of using LP signals to place quantitative constraints on the ascent rate of magma and on its pathway within the conduit is motivated by observations of rapidly increasing LP-event rate merging into the tremor before an eruption. Furthermore, the use of VLP and LP events to probe the state of the fluid and dynamic processes within a volcanic system has gained prominence in recent years (Chouet, 2003; Neuberg et al., 2000; Kumagai et al., 2003).

A number of studies have shown evidence of apparently changing source depths of tremors. Thus, tremor source location could constitute the best candidate for mapping the extend and geometry of the underlying magma, conduits, or reservoirs, and also for quantifying pressure transients caused by resonance or movement of fluids along those conduits (Battaglia et al., 2005; Di Grazia et al., 2006). There have been previous attempts to estimate the location of volcanic tremor sources mainly based on recordings from a single or a number of multichannel seismic systems (Furumoto et al., 1990; Almendros et al., 2002b; Saccorotti et al., 2004). More recently, precise locations based on amplitudes, recorded at temporary or permanent short-period vertical or 3-component broad-band stations [Bromo (Gottschammer and Surono, 2000); Piton de la Fournaise (Battaglia and Aki, 2003); Mt. Etna (Di Grazia et al., 2006)], have been performed. The latter approach is, however, inapplicable if only a few permanent stations are available.

At Mt. Etna volcano, continuous broadband seismic recordings started in November 2003, with a permanent network of 8 stations. These new broadband observations resulted in the detection of previously unobserved LP and VLP seismicity. In the following years, this network has been progressively upgraded. Since 2007, the use of 23 broad-band stations with a denser distribution around the summit craters, allowed better investigations of seismo-volcanic signals and volcano-

tectonic (VT) earthquakes together with their reliable locations. A total of 14 stations are now installed at elevations between 1100 and 3000 m a.s.l. and distances from the summit craters between 1.5 and 9 km (Fig. 1a), all equipped with Nanometrics TRILLIUM seismometers, with flat response within the 40-0.01 s period range.

In this work we present quantitative observations of seismo-volcanic signals (tremor, LP and VLP events) recorded at Mt. Etna during a 7-month period, focusing our analysis on the two powerful lava fountaining episodes recorded on September 4-5 and on November 23-24, 2007. In particular, we study the temporal evolution of the tremor and of LP-VLP activity in terms of source movement, change of the waveforms, temporal evolution of the 'dominant' resonance frequencies and the source quality factor (Q) for the LP events.

This study at Mt. Etna represents the first attempt towards continuous measurements of long-period parameters over such an extended period of time by using a high number of broad-band recordings.

2. Results

Since 2007, seismo-volcanic signals (tremor amplitude, LP and VLP events) have been routinely monitored, for surveillance purposes. In order to count LP (that also include explosion-quakes) and VLP events, an automatic detection procedure, based on the calculation of a dynamic threshold, was used. This dynamic threshold was computed as the 5^{th} percentile of power spectrum RMS of the signal filtered in frequency bands of interest. This allows the recognition and counting of the different type of events, together with an evaluation of their energy content.

The graphs (a-e) in Figure 2 show the details of tremor, LP and VLP activity in the period June 15-December 2007. The most relevant seismic feature (Figure 2 a-e), recognizable before the two lava fountaining episodes from SEC, both preceded by discontinuous ash emission and strombolian activity, is the increase in the number of LP events (Figure 2a). Also the amplitude of tremor in the LP band increases before the first eruptive episode at SEC (hereafter referred to as LF1), followed

by a progressive decrease. By contrast, the second eruptive episode (hereafter referred to as LF2) occurred in a period of decreasing tremor amplitude, even though it was preceded by a period of increasing tremor amplitude. The VLP source during this period showed a low rate of occurrence (Figure 2c). However, a temporary increase of the number of VLP events can be recognized in the second half of July before the first lava fountaining episode and after its end. Afterward, another increase in the VLP rate is recorded about one week before the onset of the second lava fountaining episode.

It is noteworthy that a low rate of VT seismicity was detected under the volcano during these months, similarly to the first half of 2007, which is in contrast with the progressively increasing rate of LP events production.

In the following paragraphs, more detailed analyses are presented on LP and VLP sources, focusing on the two lava-fountaining episodes of September 4-5 and of November 23-24. The tremor location procedure, normally applied at Etna on 1-hour-long filtered signal windows (0.5-5 Hz) for surveillance purposes (Figure 2f), has been reapplied on 5-minute-long filtered signal windows (in the frequency range 0.5-2.5 and 0.5-5 Hz) considering two wide periods encompassing the two lava fountaining episodes (shadow grey areas in Figure 2). In addition, since also LPs and VLPs may be sensitive to factors that can change with time during a magmatic cycle (Chouet, 2003), we studied and retrieved precise locations also for these signals. Approximately 1000 LPs and 700 VLPs, occurring at Mt. Etna between June 15 and December 31, were selected according to their high signal to noise ratios and analyzed.

2.1 Tremor location

In order to constrain the tremor source locations, we use the spatial distribution of tremor amplitudes as recorded by our distributed network (Figure 1a). Precise locations, based on 5-minute-long filtered signal windows, were determined for tremor recorded from August 20 to September 15, for the first lava fountaining episode, and during November 15-30, for the second

episode. Tremor source location is estimated assuming the propagation in a homogenous medium and a seismic amplitude decay with the distance (Battaglia et al., 2005; Di Grazia et al., 2006). We considered the RMS amplitudes of the 25th percentile instead of average values. This enables us to efficiently remove undesired transients in the signal and consider continuous recordings (Di Grazia et al., 2006). Tremor locations were retrieved considering two different frequency bands (0.5-2.5 Hz and 0.5- 5.0 Hz) by using a grid-search approach (Battaglia et al., 2005; Gottschammer and Surono, 2000). Then the source location of tremor is found on the basis of the goodness of the fit (R^2) obtained for each point of a 3D grid with center underneath the craters. For this grid we consider an extension of 6 x 6 km in horizontal and vertical direction, respectively, with spacing between nodes of 250 m. With the 3D grid search, we identify the most probable source locations from points where the measured amplitudes best fit the amplitude decay law for body waves. We assume as source location the centroid position of all 3D grid points whose R^2 do not differ more than 1% from the maximum R^2 (Di Grazia et al., 2006). To avoid unstable solutions, we accept a result only when: i) the goodness of the R^2 fit is = 0.9, and ii) at least 12 of the 14 stations are available. Even if the attenuation factor may not have a large influence on the source locations (Battaglia and Aki, 2003), we iteratively computed several values of the parameter α ($0 = \alpha \geq 0.4$, step 0.01) that include the quality factor, Q, with the aim of improving the goodness of the fit. We observed that the best fitting values (R^2) were achieved with very low α values, mainly between 0 and 0.02, suggesting high values of Q. For example, considering α=0.02, c=2.0 km/s and f=1Hz or 2 Hz we obtain quality factor Q values of 78 and 157, respectively. These values are in agreement with recent attenuation studies on this volcano (De Gori et al., 2005; Martinez-Arevalo et al., 2005; Giampiccolo et al., 2007), if we reasonably consider an averaged Q value for body-wave propagation in a large rock volume, that takes into account the station distances from the source (about 10 km).

Finally, in order to assess the stability of source location a Jackknife technique was employed (Efron, 1982). In Table 1, the 25th, 50th and 75th percentile of the standard error for the whole

computed Jackknife locations are reported for the period August 20 and September 15, 2007 which includes the first lava fountaining episode.

Figure 1 depicts the 3D source centroids of tremor locations computed for the period between August 20 and September 15 in the frequency range 0.5-5.0 Hz, also in order to take into account higher frequencies related to the very shallow tremor activity in proximity of the vents (Di Grazia et al., 2006). These locations reveal, for the first time, the geometry of the shallow central feeding system.

The imaged conduit consists of two connected resonating dike-like bodies, extending from sea level to the surface. The shallower dike, crossing the central craters (orange and red dots in Figure 1a-c), shows a lateral dimension changing with depth. It is located between about 1.0 km a.s.l. and the surface. In proximity of the surface it presents a maximum horizontal extension of about 2.0 km while its deeper part shows a maximum horizontal extension of about 3.0 km. Retrieved inclination and azimuth of the dike are of 15° ± 10° and 135° ± 5°, respectively, thus suggesting a resonating dike-like body striking NW-SE, slightly inclined from the vertical towards the SW.

The deeper dike (black dots in Figure 1a-c), tilted to the north of 25° and mainly located below 1 km a.s.l., shows a lateral dimension of about 3 km and a vertical extension of about 0.5 km. It strikes in the NNW-SSE direction (black dots in Figure 1 a-c) and is slightly inclined (about 20°) from the vertical towards ENE.

The stability of this shallow plumbing system geometry is confirmed considering: i) 3D source centroids of tremor locations computed during November 15-30, that include the November 23-24 lava fountaining episode at SEC and ii) tremor locations calculated on the one-hour of signals between October 2006 and December 2007, including the two lava fountaining episodes (Figure 1d). Notwithstanding the different time resolution, the locations reported in figure 1d, divided as a function of depth, show clearly the orientation of the two dike-like bodies at different depth (NNW-SSE the deeper and NW-SE the shallower).

The temporal evolution of tremor sources during August 20-September 15 indicates a progressive migration toward the SEC, starting about 8 days before the onset of the lava fountaining (Figure 3a-c), whereas a clear shallowing of sources is observed only a few hours before the onset of the lava fountaining. After its end, the source centroids migrated deeper (below 1 km a.s.l.), clustering in a wide volume, NNW-SSE oriented, beneath the central craters (black dots in Figure 1a-c and Figure 3c). Similar spatio-temporal results have also been obtained for the lava fountaining episode occurring on November 23-24.

2.2 LP-VLP classification

At Mt. Etna, LP signals are often accompanied by the VLP pulse or pulses with a peak frequency between 0.06 and 0.1 Hz. However, in some cases VLP signals occur alone, either as VLP tremor or a single VLP pulse not accompanied by an LP event (Saccorotti et al., 2007; Lockmer et al., 2007). The variability of the LP component associated to VLP events is evident in the seismogram reported in Figure 4, which shows a small VLP pulse accompanying the LP event, and then a higher VLP pulse with a much weaker LP component. LP and VLP events often occur as swarms, also with many hundreds (tens for VLP) of earthquakes within a few hours. However, VLP events usually show an almost stable low rate of occurrence (Figure 2c).

It is well known that the waveform of a seismic event depends on different effects: source effects (location and geometrical-physical-chemical features of the structure that produces the signal), propagation effects (geometrical spreading, anelastic attenuation and scattering), site effects and instrumental effects (e.g. Lay and Wallace, 1995). Therefore, two very similar waveforms imply that all these effects are the same.

On the basis of such considerations and following Green and Neuberg's procedure (Green and Neuberg, 2006), we performed a waveform classification of the LP and VLP events occurring during the period July 1 - December 31 2007, using a cross-correlation analysis between all pairs of selected signals recorded at ECPN station.

980 LP events, characterized by high signal to noise ratio and uniformly distributed in time (about 6 events per day), were selected and filtered below 0.7 Hz. The correlation matrix was obtained considering 15-second-long windows that included the whole LP events and a threshold value of cross correlation coefficient equal to 0.8 was chosen. Considering only the families with more than twenty events, we obtained three main families of LP events (hereafter referred to as family 1, 2 and 3). These families comprise about 90% of all the considered events suggesting the repetitive excitation of stationary sources in a non-destructive process. As shown in Figure 5a, most of the events belong to the family 1 (frequencies ranging between 0.3 and 0.4 Hz), except for the events occurring after the first lava fountain episode (for about 10 days) and from the second one to the end of the studied period. During these two periods most of the events belong to the family 2 showing higher frequency content (about 0.5-0.6 Hz). The family 3 (frequency of about 0.3 Hz) is instead composed of events scattered in almost the whole period.

Regarding the VLP activity, about 700 VLP events, characterized by high signal to noise ratio and uniformly distributed in time, were also selected and filtered below 0.15 Hz. Also for these events a cross correlation threshold equal to 0.8 was used. Considering only the families with more than twenty events, we obtained four main families of VLP (hereafter referred to as family 1, 2, 3 and 4; Figure 5a). The average waveforms of the four families are shown in Figure 5b. These families comprise about 85% of all the considered events suggesting also in this case the repetitive excitation of stationary sources in a non-destructive process.

2.3 Properties of the resonator system

It is known from simplified models of seismo-volcanic sources that the resonance frequency and damping of the system is strongly influenced by the nature of liquid and gas content (Chouet, 2003 and references therein). In order to study the temporal evolution of fluid-driven sources at Mt. Etna during the investigated period, we analyzed about 13000 LPs in terms of change of the source frequency and quality factor. Since the characteristic properties of a resonator system can be

estimated by the spectral features of the radiated signals, we performed two different spectral analyses on the selected LP events. Firstly, we took into account 20-second-long (2048 samples) windows, whose onset coincided with onset of the LP events. Since most of the radiated energy was concentrated below 0.7 Hz, we focused our attention on this frequency band and low-pass filtered the signal below 0.7 Hz. Then, we calculated the spectra of the vertical component of ECPN station by the Fast Fourier Transform (FFT) and obtained the highest peak frequency. Most of the calculated peak frequencies range between 0.3 and 0.7 Hz (Figure 2g).

The moving average over 25 samples (black line in Figure 2g) highlights spectral time variations, most of which are related to the volcanic activity. In fact, the frequency values decreased before the lava fountain episodes occurring on September 4-5 and November 23-24 and then increased. The decrease was slight before the first episode and strong before the second one.

In order to verify the aforementioned spectral variations and also to obtain information about the damping features of the LPs source, the Sompi analysis was applied (Chouet, 2003 and references therein). By this method of spectral analysis, a signal is deconvolved into a linear combination of coherent oscillations with amplitudes decaying and additional noise. In this approach we define a complex frequency $fc = f - ig$ where f is the frequency, g is the growth rate and i is $\sqrt{-1}$. The quality factor Q is then given by $-f/2g$. Again, we low-pass filtered the data below 0.7 Hz and obtained frequency and quality factor for autoregressive (AR) orders ranging between 2 and 10. The sharply monochromatic nature of the investigated signals justifies the choice of these low orders (Lesage, 2008). The results were very similar for all the used orders. As shown in Figure 2h, the obtained frequency values (for AR order 2) confirm the results of the FFT analysis in Figure 2g. The quality factor, mostly ranging between 2 and 8, showed an important variation after the first episode of lava fountain on September 4-5 (Figure 2i), when the values decreased from about 5 to 2-3.

2.4 LP and VLP location

LP locations were performed by applying the semblance technique (Neidel and Tarner, 1971). This method was preferred to the radial semblance technique (Kawakatsu et al., 2000), used instead for the VLPs analysis, because the particle motion of the observed LPs was radial at only some summit stations. According to their uniform distribution in time and high signal-to-noise ratios, a subset of about 900 LPs were selected and located by using the five or six nearest stations to the summit area. Four-second-long windows of seismic data, low-pass filtered below 0.7 Hz, whose onset coincided with onset of the LP events, were used. For the locations a 3D grid is adopted, with dimensions of 6×6 km and vertical extent of 3.25 km (from 0 km a.s.l. to the top of the volcano). The horizontal and vertical grid spacing is 125 m. A value of 1.7 km/s was chosen as seismic velocity because it allowed to obtain the maximum semblance value. This value is consistent with seismic velocity values reported in literature for this kind of study at Mt. Etna (e.g. Privitera et al., 2003; Gresta et al., 2004; Bean et al., 2008). Furthermore, the most recent high-resolution velocity tomographies on this volcano suggest that, for depth less than 1.0-1.5 km (Cocina et al., 2008), the used value is reliable and justified by the presence of intensely fractured rocks and pyroclastic deposits in the shallow layers of the volcanic edifice.

The results, summarized in Figure 6 suggest shallow LP sources located below the summit craters. The LP source showed striking time variations and a deepening from 3 to 1 km a.s.l. after the two lava fountain episodes. In addition, the LP source gradually shifted northward from September to November.

Concerning the VLP seismicity, about 400 VLP events occurring between July and October 2007, were located by the radial semblance method (Kawakatsu et al., 2000). Because of the low amplitude of these signals, we located the VLP source by using only the four stations nearest to the summit area. The lack of one of the closest stations (EPDN; Figure 1) between November and December precluded the extension of the analysis to the period of the November 23-24 lava fountaining episode. 20-second-long windows of seismic signal, whose onset coincided with the

onset of the VLP events, low-pass filtered below 0.15 Hz, were used. The 3D grid is the same as the one used to locate the LP events.

The VLP locations, shown in Figure 6, also suggest for VLP seismicity shallow sources located just below the summit area. Unlike the LP locations, the VLP locations (Figure 6) remain steady for the whole period. A slight deepening can be observed after the lava fountain episode occurring on September 4-5. In order to estimate the error of the location, we followed the Almendros and Chouet method (Almendros and Chouet, 2003). It is noteworthy that in most cases the obtained error region contained only the node of the grid characterized by the maximum semblance value. Therefore, if error bars are not reported, the error can be considered lower than the grid spacing.

It is noteworthy that, the used location methods do not take into account material heterogeneity and topography. The former can affect the location results of both semblance and radial semblance methods. Conversely, the latter mostly influences the locations obtained by radial semblance, that is based on whether the similarity of the waveform or the particle motion. However results obtained during a recent large-scale passive seismological experiment (June-July 2008), aimed at complementing the permanent Etna monitoring system in the near-field, with the deployment of over 20 broad-band stations in summit area, showed that the LP and VLP source locations obtained by only the permanent stations are quite reliable (Patanè et al., 2008). For both LP and VLP sources, locations obtained using the dense network were only shifted by about 100-200 m However, for seismo-volcanic studies it is important to deploy as many stations as is feasible close to the source with the best azimuthal coverage possible as suggested by Neuberg and Pointer (2000), which we believe allows partially minimizing the above mentioned effects.

3. Discussion and conclusion

A first study on Mt. Etna's LPs activity, recorded from November 2003 until the onset of the 2004 summit effusive eruption, suggested the lack of a link between the LP activity and the

eruption (Saccorotti et al., 2007). More recent analysis has suggested the existence of this possibility (Lockmer et al., 2008).

In this study, we have analyzed the temporal evolution of volcanic tremor, LPs and VLPs activity which occurred at Etna from June to December 2007, thus encompassing two powerful lava fountaining episodes taking place on September 4-5 and on November 23-24 from SEC.

The most important results here obtained concern:

1) The discovery of the magma pathway geometry feeding the eruptive activity at SEC, highlighted by precise volcanic tremor source locations obtained in wide periods including the two lava fountaining episodes. The imaged plumbing system consists of two connected resonating dike-like bodies, NNW-SSE and NW-SE oriented, extending from sea level to the surface. The stability in recent times of this shallow plumbing system geometry, was confirmed by considering the October 2006 - December 2007 period (Figure 1d). The NW-SE trending source region has recently been supported by: i) the moment-tensor inversion of LPs sources, indicating a crack-like geometry (Lockmer et al., 2007) and ii) the most recent dike propagation trends modeled by crustal deformation data (Bonaccorso and Davis, 2004; Patanè et al., 2005). Further evidence for NNW-SSE and NW-SE dyke structures can be found at the surface, having been exposed by erosion nearby the summit craters. Their presence to depths of 500-700 m is displayed in a very impressive manner in the southern wall of the Valle de1 Bove (see rose diagram of dikes direction in Figure 1a).

2) The evidence of time variations of volcanic tremor, LP and VLP events, that accompany eruptive activity and that can be explained by transport/discharge of gas-rich magma.

In the medium-term, the clearest relationship between the uprising of magma, the progressive increase of the pressure in the conduits and the renewal of activity at SEC (INGV-CT volcanological reports at http://ct.ingv.it) can be recognized since July 15 by the increasing activity of LPs events. Afterward, since August 15 the start of a discontinuous activity of ash emission followed by strombolian activity at SEC (Andronico et al., 2008b) on August 27, was accompanied

by: 1) the migration of tremor sources at shallow depth (Figure 2f); 2) the progressive increase in the tremor amplitude (Figure 2 e); 3) the increase in the number of LPs and of its associated energy (Figure 2a,b) and 4) by variations of ground deformation measurements. In fact, ground deformation measured by GPS stations at the summit (in Figure 2l the baseline ECPN-EPDN is shown) indicated an accelerating small dilatation of the summit area. A low rate of seismicity was, instead, detected under the volcano during these months, similarly to the first half of 2007, suggesting that magma flowed almost aseismically, without any significant generation of VT quakes.

These observations suggest that, since August 15, the arrival of a small batch of undegassed magma (Nishimura, 2006) might have played a significant role in the re-activation of the SEC, leading to the September 4-5 lava fountaining episode. After this eruptive episode, the observed deflation of the edifice (Figure 2l) and changes in tremor locations (deepening; Figure 2f) and LP event signatures (mild increase in frequency peak of tremor and faster decay of LPs; Figure 2i), can easily be explained by the gas-rich magma discharge during the paroxysm and the consequent decrease of gas-volume fraction in the magma/gas mixture (Thompson et al., 2002; Kumagai, 2006). The cartoon in Fig. 7 illustrates the evolution of the eruptive activity at SEC, leading to this lava fountaining episode, between July and September 2008.

Afterward, a new slow magma recharge affected the conduit, as testified by a similar but slightly different behavior of GPS ground deformation and variations in seismo-volcanic parameters, which prepared the way for the November 23-24 lava fountaining episode.

In the short-term, the decrease and following increase of the 'dominant' frequency of the LP events occurring before and after the two lava fountain episodes can be explained by variations of the resonator system. It is noteworthy that, the first eruptive episode was also followed by a quality factor decrease.

We can assume that the resonator system, source of LPs, is represented by a fluid-filled crack as suggested by recent studies based on the waveform inversion (Kumagai et al., 2003; Lockmer et al.,

2007). Moreover, as suggested by the strong and frequent explosive activity involving discharge of high volumes of magma during the studied time period, the fluid can reasonably be considered a magma-gas mixture. Therefore, in the light of these assumptions, the aforementioned variations that followed the lava fountain episodes may be due to a decrease in the solid/fluid impedance contrast caused by either a decrease of the gas-volume fraction in the fluid or by an increase of pressure at constant temperature and gas-volume fraction (Kumagai, 2006). The observed eruptive activity supports the first interpretation that, in fact, is consistent with the gas/gas-rich magma discharge during the lava fountain episodes. Similarly, the decrease of the 'dominant' frequency, observed before the lava fountain episodes, can be interpreted as the consequence of an increase of the gas-volume fraction in the fluid. This variation, therefore, can likely be linked to the fast uprise of gas-rich magma preceding the explosive activity. It is noteworthy that the interpretation of the quality factor variations implies that the attenuation due to intrinsic losses is negligible.

Concerning the LP and VLP source locations, it is worth noting that the observed limited and stable spatial extension of the most active clusters of LP events can be recognized over the years (Saccorotti et al., 2007; Lockmer et al., 2008). This is indicative of the repetitive action of non-destructive sources in a restricted source zone where a shallow crack or a system of cracks probably exists. At Mt. Etna VLP earthquakes, similar to those observed in other active volcanoes (e.g. Kilauea, Hawaii), have dominant spectral peaks at periods of 10-15 seconds and can be associated with the transport of magma or gas slugs through cracks. As shown in Figures 6b and 6d, the cluster of VLP lies directly beneath the main cluster of LP seismicity. This can be explained if VLP and LP oscillations originate in the same system, representing the volumetric deformation and LP oscillation of a shallow crack (or plexus of cracks), respectively (Chouet, 2003).

Conversely, the scattered sources of deeper LPs and volcanic tremors would represent the result of the dynamic interaction of volcanic fluids (magma degassing) with surrounding solid rocks in wider parts of conduit.

In conclusion, our results confirm the feasibility of volcanic tremor and LPs location as an effective monitoring tool for tracking the temporal evolution of seismo-volcanic sources and the ascent of small magma gas-rich batches which could flow almost aseismically through the conduits. This study, integrated with geodetic observations, may be useful to forecast eruptions that, like the summit effusive or explosive eruptions at Mt. Etna, apparently do not show clear precursor signals.

Acknowledgments

We thank M. Mattia for ground deformation GPS data. Supported by grants from the European Union VOLUME FP6-2004-Global-3. Comments from Joshua Jones, Thomas Walter and the anonymous Associate Editor helped greatly to improve the manuscript.

References

Allard, P., B. Behncke, S. D'Amico, M. Neri, and S. Gambino (2006), Mount Etna 1993–2005: Anatomy of an evolving eruptive cycle, *Earth-Science Rev.*, *78*, 85-114.

Almendros, J., B. Chouet, P. Dawson, and T. Bond (2002a), Identifying elements of the plumbing system beneath Kilauea Volcano, Hawaii, from the source locations of very-long-period signals, *Geophys. J. Int.*, *148*, 303-312.

Almendros, J.B., B. Chouet, P. Dawson, and C. Huber (2002b), Mapping the sources of the seismic wavefield at Kilauea volcano, Hawaii, using data recorded on multiple seismic antennas, *Bull. Seism. Soc. Am.*, *92*, 2333-2351.

Almendros, J., and B. Chouet (2003), Performance of the radial semblance method for the location of very long period volcanic signals, *Bull. Seism. Soc. Am.*, *93*, 1890-1903.

Andronico, D., A. Cristaldi, D. Lo Castro, S. Scollo, and J. Taddeucci (2007), The 24 November 2006 paroxysm at south-east crater, Mt. Etna, *Proceedings of the XXIV General Assembly of the IUGG*, Perugia July 2-13, 2007.

Andronico, D., S. Scollo, S. Caruso, and A. Cristaldi, (2008a), The 2002–03 Etna explosive activity: Tephra dispersal and features of the deposits, *J. Geophys. Res.*, *113*, B04209 doi: 10.1029/2007JB005126.

Andronico, D., A. Cristaldi, and S. Scollo (2008b), The 4–5 September 2007 lava fountain at South-East Crater of Mt Etna, Italy, *J. Volcanol. Geotherm. Res.*, *173*, 325-328.

Battaglia, J., and K. Aki (2003), Location of seismic events and eruptive fissures on the Piton de la Fournaise volcano using seismic amplitudes, *J. Geophys. Res.*, *108*, B8, 2364.

Battaglia, J., K. Aki, and V. Ferrazzini (2005), Location of tremor sources and estimation of lava output using tremor source amplitude on the Piton de la Fournaise volcano: 1. Location of tremor sources, *J. Volcanol. Geotherm. Res.*, *147*, 268-290.

Bean, C., I. Lockmer, and G. O'Brien (2008), Influence of near-surface volcanic structure on long-period seismic signals and on moment tensor inversions: Simulated examples from Mount Etna, *J. Geophys. Res.*, *113*, doi:10.1029/2007JB005468.

Behncke, B., and M. Neri (2003), Cycles and trends in the recent eruptive behavior of Mount Etna (Italy), *Can. J. Earth Sci.*, *40*, 1405–1411.

Bonaccorso, A., and P.M. Davis (2004), Modeling of ground deformation associated with recent lateral eruptions: mechanics of magma ascent and intermediate storage at Mt. Etna, in *Mt.Etna: Volcano Laboratory*, edited by Bonaccorso A et al., 293-306, AGU Geophysical Monograph Series 143.

Chouet, B. (1996), Long-Period volcano seismicity: its source and use in eruption forecasting, *Nature*, *380*, 309-316.

Chouet, B. (2003), Volcano seismology, *Pure. App. Geophys.*, *160*, 739-788.

Cocina, O., G. Barberi, and D. Patanè (2008), The Mt Etna 2001-2003 eruptive period: the seismological point of view, *General assembly IAVCEI Reykjavik August 2008*.

Del Carlo, P., L. Vezzosi, and M. Coltelli (2004), Last 100 ka tephrostratigraphic record of Mount Etna, in *Mt. Etna: Volcano Laboratory*, edited by Bonaccorso A. et al., 77-89, AGU Geophysical Monograph Series 143.

De Gori, P., C. Chiarabba, and D. Patanè (2005), Qp structure of Mt. Etna: constraints for the physics of the plumbing system. Journal of Geophysical Research, *J. Geophys. Res, 110*, B05303, doi: 10.1029/20033JB002875.

Di Grazia, G., S. Falsaperla, and H. Langer (2006), Volcanic tremor location during the 2004 Mount Etna lava effusion, *Geophys. Res. Lett., 33*, L04304, doi:10.1029/2005GL025177.

Efron, B. (1982), *The Jackknife, the Bootstrap and Other Resampling*, Plans. Soc. for Ind. and Appl. Math., Soc. for Ind. and Appl. Math., Philadelphia.

Furumoto, M., K Takahiri, H. Inoue, I. Yamada, K. Yamaoka, A. Ikami, and Y. Fukao (1990), Twin sources of high-frequency volcanic tremor of Izu-Oshima volcano, Japan, *Geophys. Res. Lett., 17*, 25-27.

Giampiccolo, E., S. D'Amico, D. Patanè, and S. Gresta (2007), Attenuation and source parameters of shallow microearthquakes at Mt. Etna Volcano, Italy, *Bull. Seism. Soc. Am., 97*, 184-197.

Gottschammer, E., and I. Surono (2000), Locating tremor and shock sources recorded at Bromo volcano, *J. Volcanol. Geotherm. Res., 101*, 199-209.

Green, D., and J. Neuberg, (2006), Waveform classification of volcanic low-frequency earthquake swarms and its implication at Soufrière Hills Volcano, Monserrat, *J. Volcanol. Geotherm. Res., 153*, 51-63.

Gresta, S., M. Ripepe, E. Marchetti, S. D'Amico, M. Coltelli, A.J.L. Harris, and E. Privitera (2004), Seismoacoustic measurements during the July-August 2001 eruption of Mt. Etna volcano, Italy, *J. Volcanol. Geotherm. Res., 137*, 219-230.

Jaupart, C., and S. Vergniolle (1988), Laboratory models of Hawaiian and Strombolian eruptions, *Nature, 331*, 58-60.

Kawakatsu, H., S. Kaneshima, H. Matsubayashi, T. Ohminato, Y. Sudo, T. Tsutsui, K. Uhira, H. Yamasato, H. Ito, and D. Legrand (2000), Aso94: Aso Seismic Observation with Broadband Instruments, *J. Volcanol. Geotherm. Res.*, *101*, 129-154.

Kumagai, H., K. Miyakawa, H. Negishi, I. Hiroshi, K. Obara, and D. Suetsugu (2003), Magmatic dike resonances inferred from Very-Long-Period seismic signals, *Science*, *299*, 2058-2061.

Kumagai, H. (2006), Temporal evolution of a magmatic dike system inferred from the complex frequencies of very long period seismic signals, *J. Geophys. Res.*, 111, B06201.

Lay, T., and T.C. Wallace (1995), *Modern global seismology*, Academic Press, San Diego, California, 521 pp.

Lesage, P. (2008), Automatic estimation of optimal autoregressive filters for the analysis of volcanic seismic activity, *Nat. Hazards Earth. Syst. Sci.*, *8*, 369-376.

Lockmer, I., C.J. Bean, G. Saccorotti, and D. Patanè (2007), Moment-tensor inversion of LP events recorded on Etna in 2004 using constraints obtained from wave simulation tests, *Geophys. Res. Lett.*, *34*, L22316, doi:10.1029/2007GL031902.

Lockmer, I., G. Saccorotti, B. Di Lieto, and C.J. Bean (2008), Temporal evolution of long-period seismicity at Etna volcano, Italy, and its relationships with the 2004-2005 eruption, *Earth Planet. Sci. Lett.*, *266*, 205-220.

Martinez-Arevalo, C., D. Patanè, A. Rietbrock, and J.M. Ibanez (2005), The intrusive process leading to the Mt. Etna 2001 flank eruption: Constraints from 3-D attenuation tomography, *Geophys. Res. Lett.*, *32*, L21309, doi:10.1029/2005GL023736.

Neidel, N., and M.T. Tarner (1971), Semblance and other coherency measures for multichannel data, *Geophysics*, *36*, 482-497.

Neuberg, J., and T. Pointer (2000), Effects of volcano topography on seismic broad band waveforms *Geophys. J. Int.*, *143*, 239–248.

Neuberg, J., R. Luckett, B. Baptie, and K. Olsen, (2000), Models of tremor and low-frequency earthquake swarms on Montserrat, *J. Volcanol. Geotherm. Res.*, *101*, 83-104.

Nishimura, T. (2006), Ground deformation due to magma ascent with and without degassing, *Geophys. Res. Lett.*, *33*, L22309, doi:10.1029/2006GL028101.

Patanè, D., P. De Gori, C. Chiarabba, and A. Bonaccorso (2003), Magma ascent and the pressurization of Mt. Etna's volcanic system, *Science*, *299*, 2061-2063.

Patanè, D., M. Mattia, and M. Aloisi (2005), Shallow intrusive processes during 2002–2004 and current volcanic activity on Mt. Etna, *Geophys. Res. Lett.*, *32*, L06302.

Patanè, D., G. Barberi, O. Cocina, P. De Gori, and C. Chiarabba (2006), Time-resolved seismic tomography detects magma intrusions at Mount Etna, *Science*, *313*, 821-823.

Patanè, D., C. Bean, J-P Metaxian, G. Saccorotti, F. Bianco, G. Di Grazia, A. Cannata, P. Montalto, L. Zuccarello, and ETNAVOL08 Scientific Group (2008), Understanding the seismo-volcanic sources by a dense broad-band passive seismic experiment during the 2008 Mt. Etna eruption, *in preparation*.

Privitera, E., T. Sgroi, and S. Gresta (2003), Statistical analysis of intermittent volcanic tremor associated with the September 1989 summit explosive eruptions at Mount Etna, Sicily, *J. Volcanol. Geotherm. Res.*, *120*, 235-247.

Saccorotti, G., L. Zuccarello, E. Del Pezzo, J. Ibanez, and S. Gresta (2004), Quantitative analysis of the tremor wavefield at Etna volcano, Italy, *J. Volcanol. Geotherm. Res.*, *136*, 223-245.

Saccorotti, G., I. Lockmer, C.J. Bean, G. Di Grazia, G., and D. Patanè (2007), Analysis of sustained long-period activity at Etna Volcano, Italy, *J. Volcanol. Geotherm. Res.*, *160*, 340-354.

Sahagian, D. (2005), Volcanic eruption mechanisms: insights from intercomparison of models of conduit processes, *J. Volcanol. Geotherm. Res.*, *143*, 1-15 .

Thompson, G., S.R. McNutt, and G. Tytgat (2002), Three Distinct Regimes of Volcanic Tremor Associated with Eruptions of Shishaldin Volcano, Alaska, April 1999, *Bull. Volcanol.*, *64*, 535-547.

Woods, A.W., and S.S.S. Cardoso (1997), Bubble–melt separation as a trigger for basaltic volcanic eruptions, *Nature*, *385*, 518-520.

Table

	25^{th} percentile	50^{th} percentile	75^{th} percentile
Latitude	0.39	0.46	0.54
Longitude	0.48	0.55	0.62
Depth	0.65	0.77	0.88

Table 1. Standard error in Km for Latitude, Longitude and Depth of the Jackknife estimation.

Figures

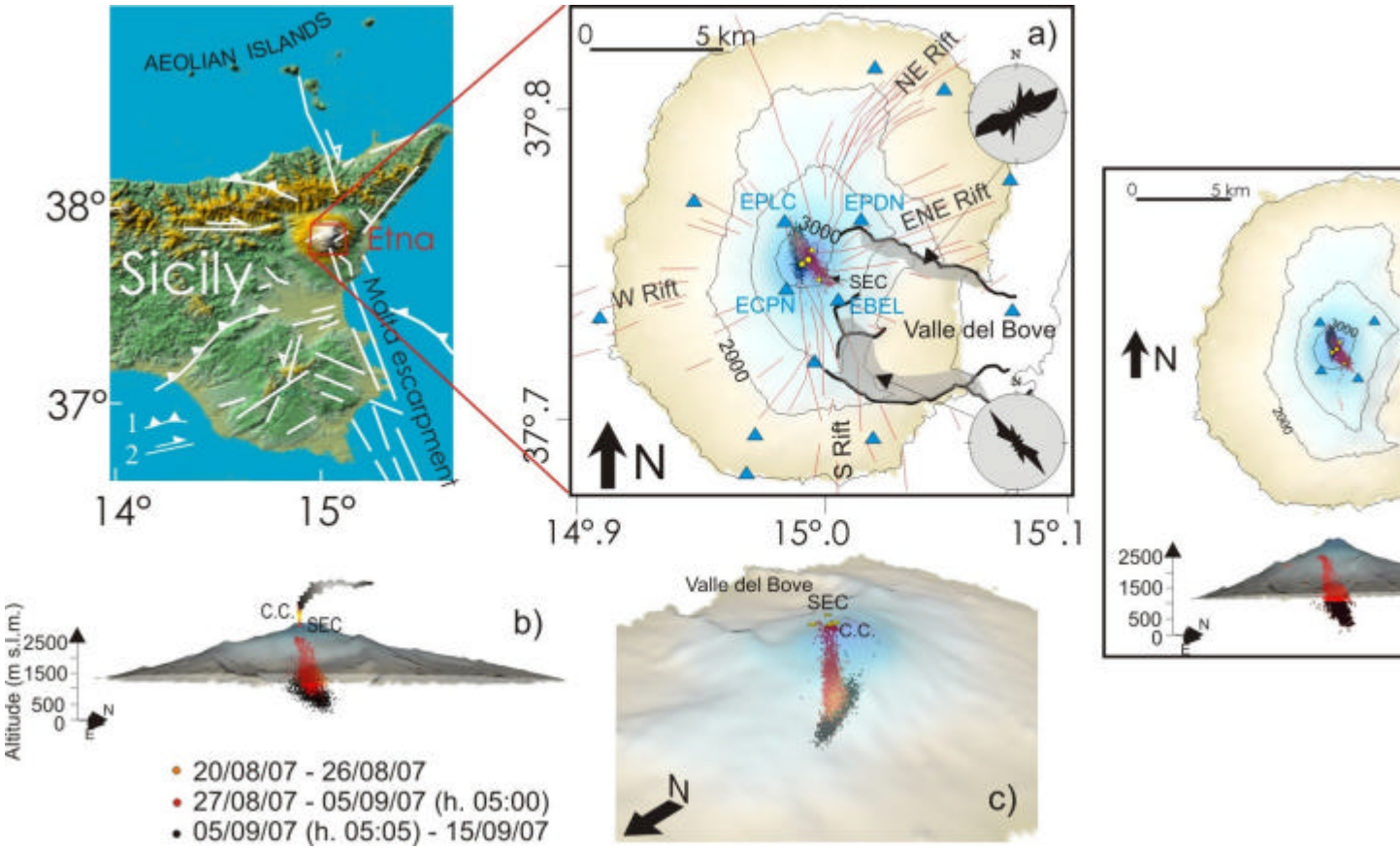

Fig. 1. **Top left)** Structural map of eastern Sicily reporting: 1. the front of the Appenninic-Maghrebian chain and 2. the main faults. **a)** Map of the summit part of Mt. Etna volcano showing 3D source centroids of volcanic tremor locations computed between August 20 and September 15, 2007. In the map, broad-band seismic stations (light blue triangles) operating during the study period and used for tremor locations, the GPS stations used in this work (ECPN and EPDN, that are located at the same place as the homonymous seismic stations), historical eruptive fissures (red lines) and time evolution of tremor locations (orange, red and black circles), are also reported. The concentric black curves represent elevation contours at 500-m intervals. Yellow dots indicate central craters (C.C.). The rose diagrams show the dyke structure directions as appearing at the surface through erosion processes in the southern and northern walls of Valle de1 Bove. **b,c)** 3D images of the volcanic edifice reporting volcanic tremor locations. **d)** 3D source centroids of volcanic tremor locations computed between October 2006 and December 2007, separated into two classes of depth (black dots = 1000 m and red dots > 1000 m).

.

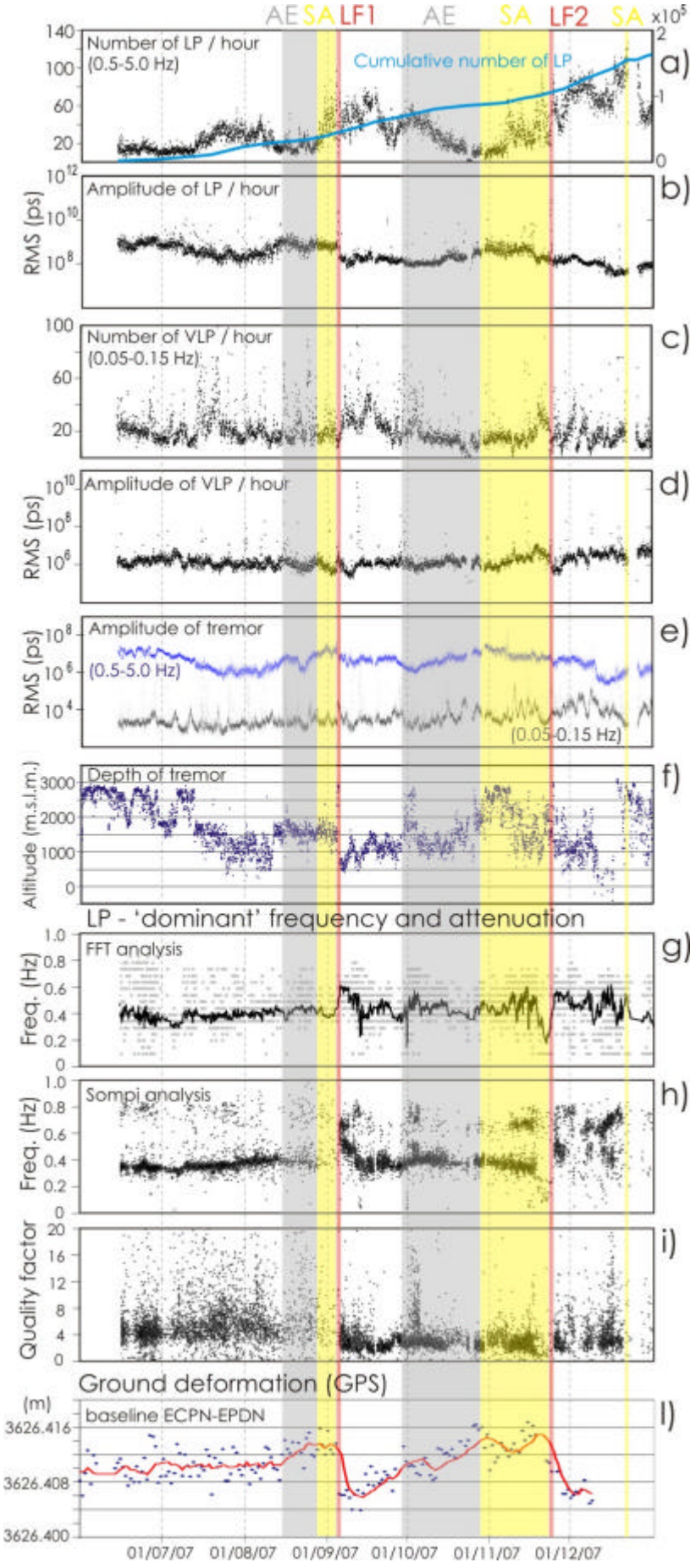
AE SA LF1 AE SA LF2 SA
Number of LP / hour (0.5-5.0 Hz)
Cumulative number of LP
a)
Amplitude of LP / hour
RMS (ps)
b)
Number of VLP / hour (0.05-0.15 Hz)
c)
Amplitude of VLP / hour
d)
Amplitude of tremor
(0.5-5.0 Hz)
(0.05-0.15 Hz)
e)
Depth of tremor
Altitude (m.s.l.m.)
f)
LP - 'dominant' frequency and attenuation
FFT analysis
Freq. (Hz)
g)
Sompi analysis
h)
Quality factor
i)
Ground deformation (GPS)
(m)
baseline ECPN-EPDN
l)
01/07/07 01/08/07 01/09/07 01/10/07 01/11/07 01/12/07

Fig. 2. Temporal variation of the seismo-volcanic activity at ECPN station and GPS ground deformation in the period June – September 2007. **a,c)** Number of LP and VLP per hour and **b,d)** related RMS values (energy content), **e)** tremor amplitude computed in the LP and VLP bands, **f)** tremor depth, **g-i)** 'dominant' frequency and quality factor of LP, and **l)** GPS ground deformation measurements in the summit area (baseline between ECPN and EPDN GPS stations). The vertical red lines mark the two lava fountaining episodes of September 4-5 and November 23-24. The shadow grey area marks the period of discontinuous ash emission, whereas the yellow one marks the period of prevalent strombolian activity. The red line in l) represents the moving average of original data considering groups of 5 measurements.

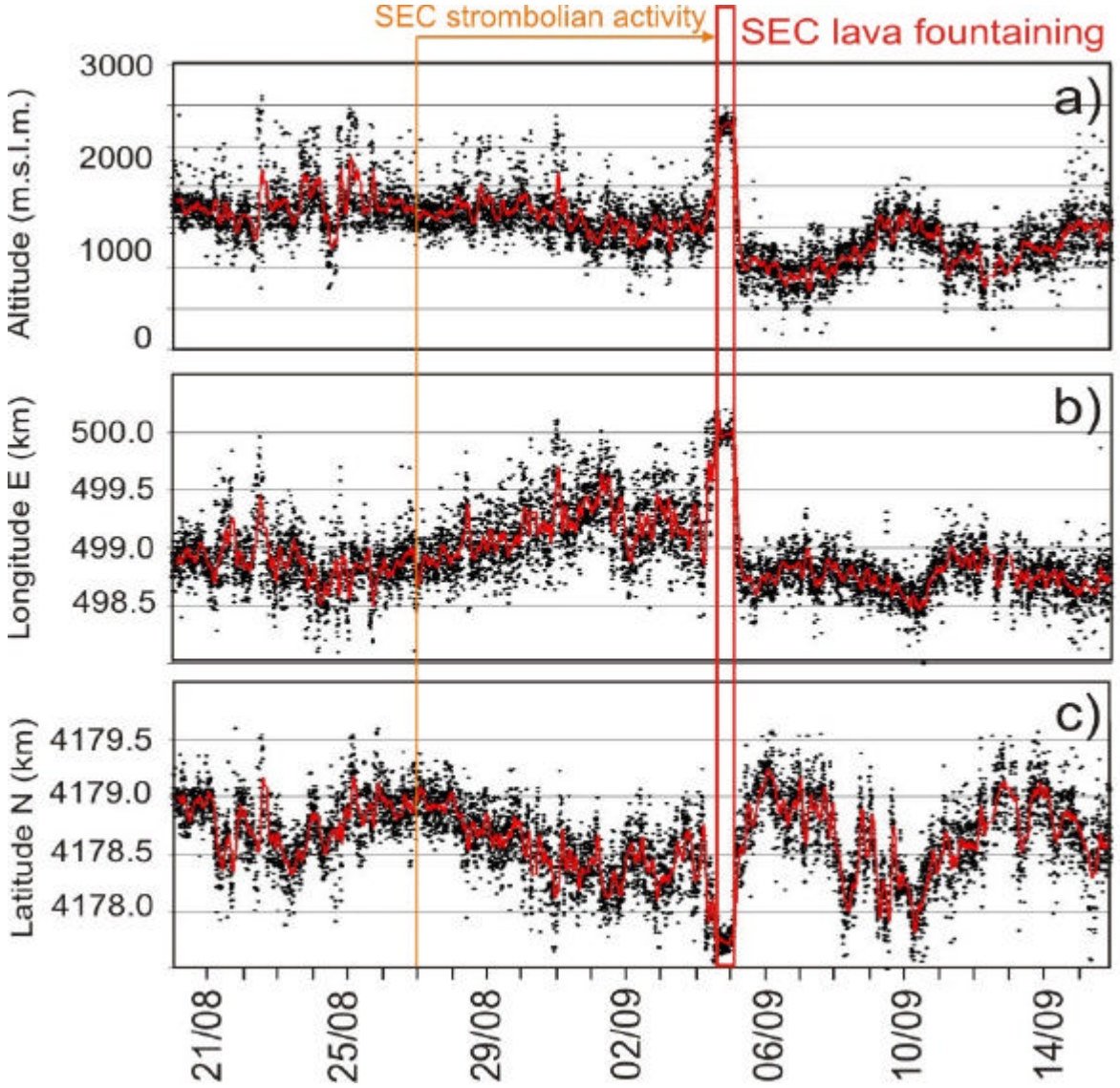

Fig. 3. Temporal evolution between August 20 and September 15 of altitude **(a)**, longitude **(b)** and latitude **(c)** of tremor sources. The red lines are the moving average of original data considering groups of 30 measurements. The vertical orange line marks the start of strombolian activity at SEC, while the empty red rectangle defines the lava fountaining period (for details see INGV-CT volcanological reports at http://ct.ingv.it).

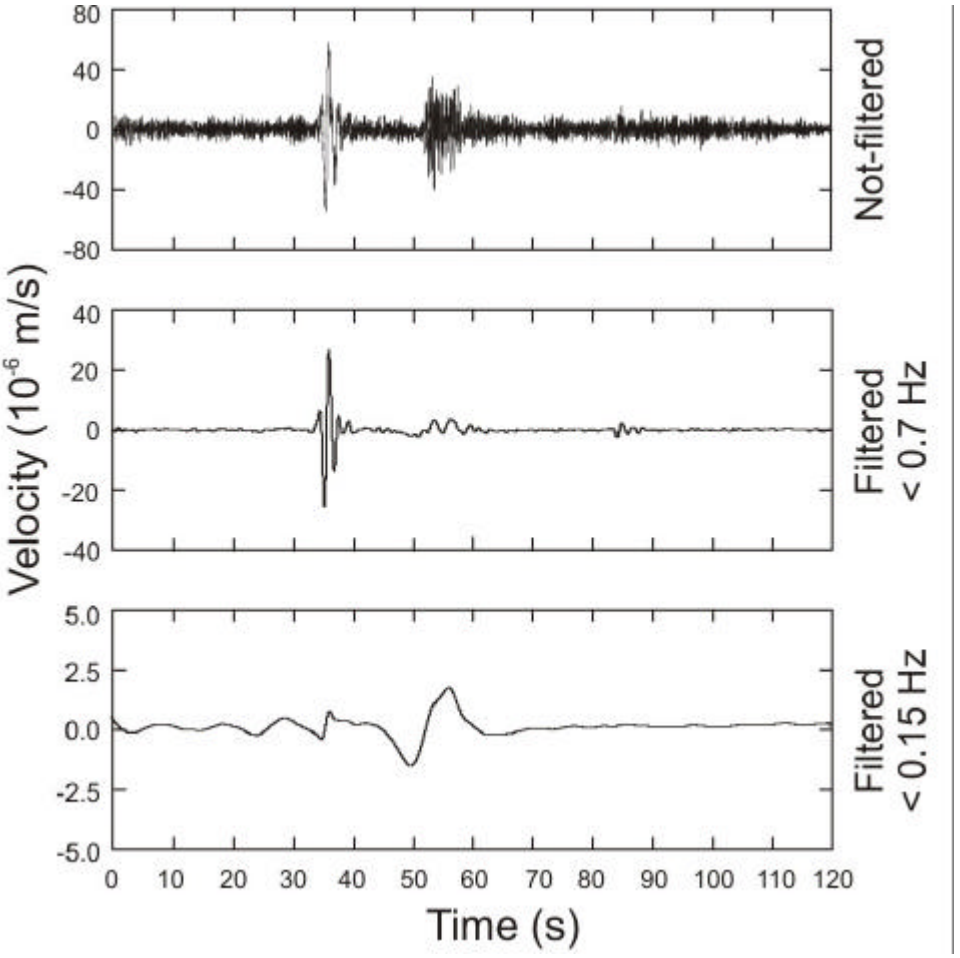

Fig 4. Velocity seismogram recorded at the vertical component of ECPN station on September 7, 2007. The low-pass filtered signals, below 0.7 Hz and 0.15 Hz, are also reported.

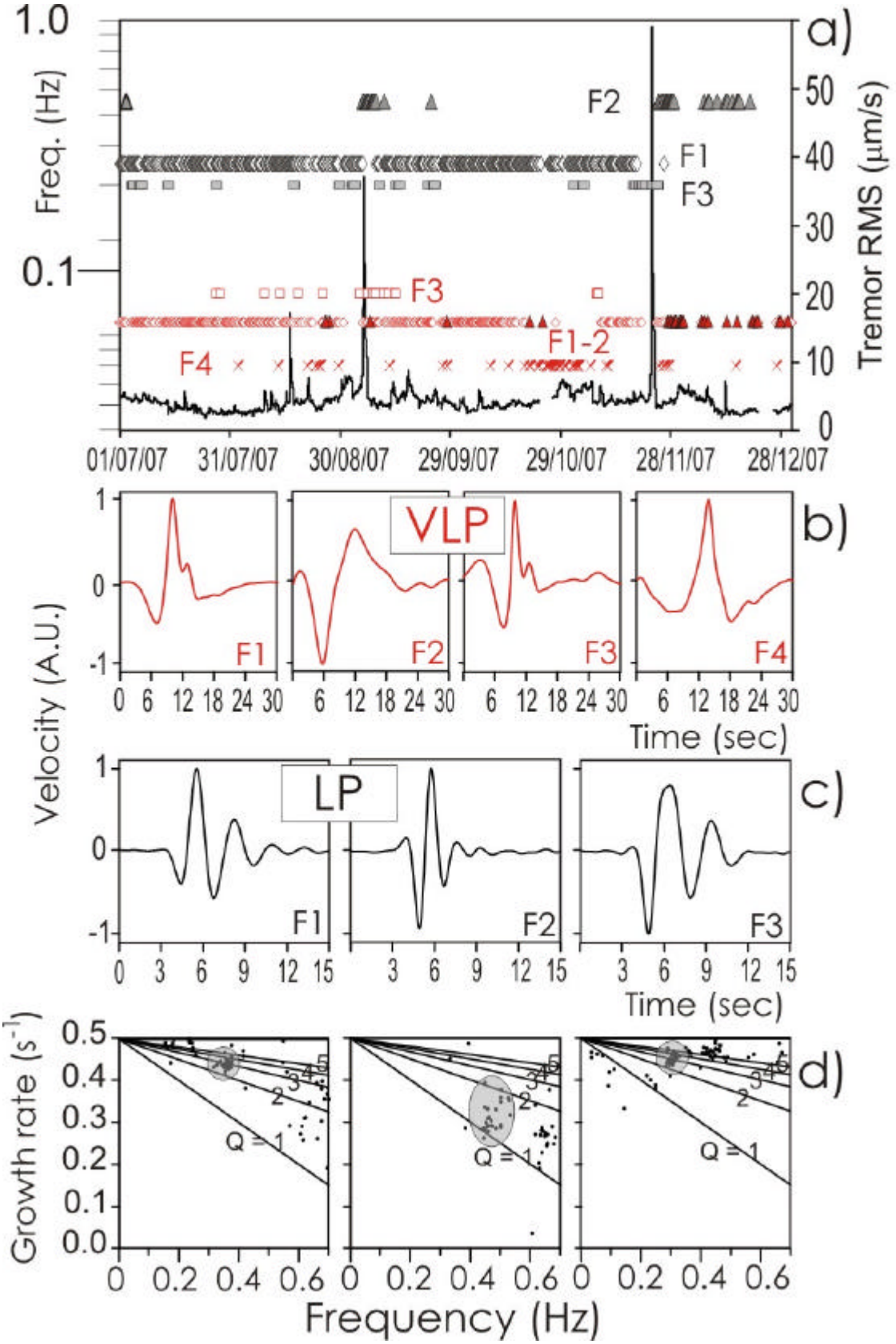

Fig. 5. **a)** Time distribution of the LP [Family 1 (black diamonds), 2 (black triangles) and 3 (black squares)] and VLP [Family 1 (red diamonds), 2 (red triangles), 3 (red squares) and 4 (red crosses)] events as a function of their average frequency content, and RMS of the tremor signal calculated by

30-minute-long time windows at the vertical component of ECPN station (black line). **b)** Average waveforms of the four VLP families and **c)** of the three LP families. **d)** *f-g* diagrams of the average waveforms shown in c). The black lines represent values of constant quality factor (Q). Clusters of points (encircled with grey ellipses) indicate a resolved dominant mode, scattered points represent noise.

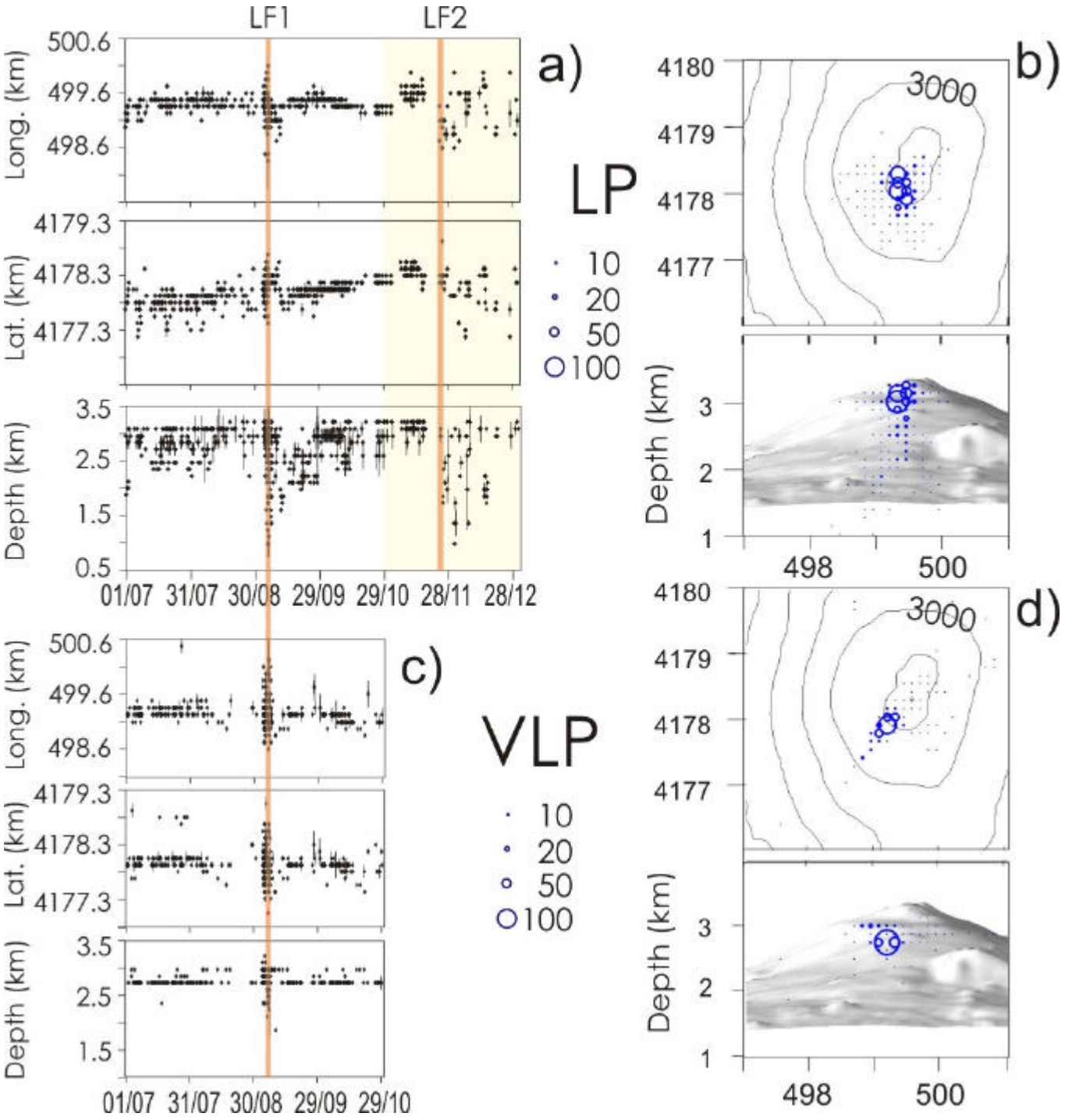

Fig. 6. **a,c)** Time variation of the source location of about 900 LP and 400 VLP events, occurring between 1 July and 31 December 2007 and between 1 July and 31 October 2007, respectively. The yellow rectangle indicates the time period when EPDN station did not operate. **b,d)** Maps and W-E sections of summit area with the source locations of the LP (b) and VLP (d) events (blue dots). The radii of the dots are proportional to the number of the locations in each grid node (see blue dots and numbers reported at center).

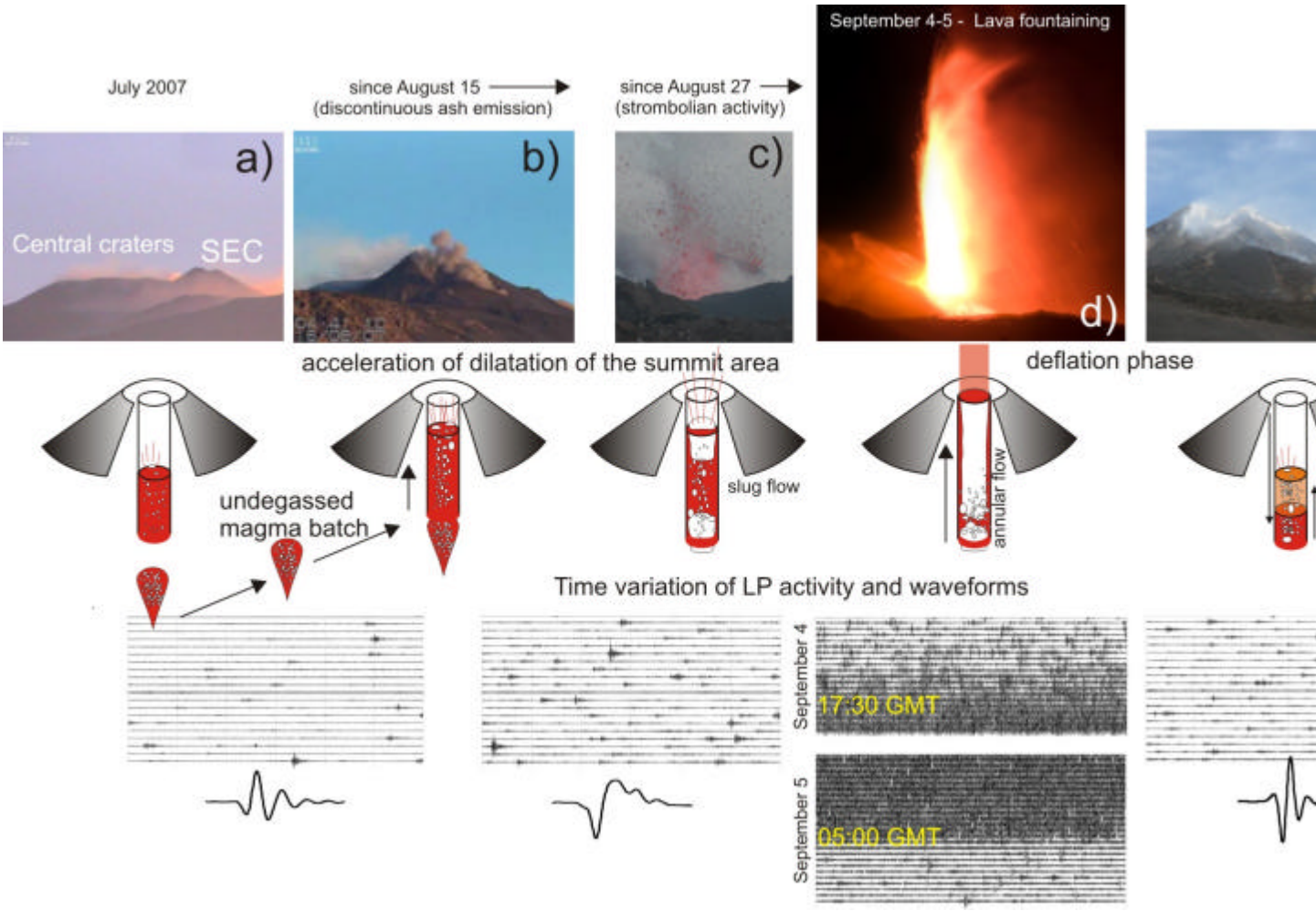

Fig, 7 a,e) Cartoon showing the evolution of eruptive activity at the SEC between July and September 2007. Here the increase in the magma rising rate and volatile flux is considered the most probable trigger of the formation of the September 4-5 fire fountain through a progressive coalescence of bubbles in the conduit. b) In a first stage, since August 15, a discontinuous activity of episodic ash puff was observed, mainly consisting of lithic material, indicating failure and collapses of the inner walls of the conduit (Andronico et al., 2008b). This emission gradually increased in frequency and intensity and was then replaced by the ejection of incandescent material. c) From August 27 strombolian activity (formation and release of gas slugs) started, becoming more regular and stronger in the next days. d) The increasing gas volume fraction in the conduit modified the slug flow (strombolian activity) into an annular flow responsible for the 4-5 September lava fountain, driven by a long inner gas jet. e) After the eruptive episode, accompanied by a deflation

phase, the observed fluctuation in the depth of tremor locations (Fig. 3a) could suggest oscillation in the magma level in the conduits. Several geophysical variations have been recognized both in the medium- and short-time during the considered period (see text for further details). Some examples of seismograms showing the increase in the LP activity and the main changes in the LP waveforms are also shown.